A technique for phase-detection auto focus under near-infrared-ray incidence in a back-side illuminated CMOS image sensor pixel with pyramid textured interfaces for diffraction

Tatsuya Kunikiyo, Yotaro Goto, Fumitoshi Takahashi, Hidenori Sato, Takeshi Kamino,
Koji Iizuka, Yutaka Akiyama and Tomohiro Yamashita
Renesas Electronics Corporation
751 Horiguchi, Hitachinaka, Ibaraki, 312-8504, Japan
Phone: +81-29-272-3111 (ex.3485) E-mail: tatsuya.kunikiyo.zn@renesas.com

Abstract

A novel phase-detection auto focus (PDAF) technique for incident 850 nm plane wave is demonstrated using 400 nm base size inverted pyramid textured interfaces for diffraction (PTID) and deep trench isolation (DTI), which are locally arranged on light receiving surface (LRS) of crystalline silicon (c-Si). No metal light shielding film (LSF) for pupil division is formed. The key concept of this work for PDAF is to perform the pupil division by generating light trapping selectively in a pixel according to incident angle. The present pixel is based on a back-side illuminated CMOS image sensor pixel; the pixel pitch is 1.85 μm and the thickness of c-Si is around 3 μm. The simulation, based on three-dimensional finite difference time domain (3D-FDTD) method, shows that the external quantum efficiency (EQE) of the present pixel exhibits above 36.8 % with the maximum of 54.2 % for incident angles of -30° to +30°, owing to the selective light trapping; it exhibits 2.9 times improvement in the EQE at normal incidence compared to that of current state-of-the-art pixel with a flat LRS and half metal-shielded aperture; the EQE is 40.3% and 13.8 %, respectively. The present technique can enhance the accuracy of AF under low-illuminated condition.

Introduction

The demand for auto focus in night vision photography requires a technique for phase-detection auto focus (PDAF) to capture near infrared radiation. To achieve a high accuracy of PDAF under low-illuminated condition, it is desired to increase external quantum efficiency (EQE) in a pixel for PDAF fabricated on a cost-effective crystalline silicon (c-Si) substrate.

In a pixel for PDAF, a light shielding film (LSF) for limiting light incident on an on-chip micro lens is provided [1], and the amount of light incident on the image pickup element is limited, so that the sensitivity is deteriorated. As a result, accuracy of detection of the focal position may be lowered. Moreover, an absorption coefficient in c-Si at a wavelength of 850 nm is almost one order of magnitude smaller than that at a wavelength of 550 nm [2]. While it is possible to obtain a higher EQE by simply having a thicker c-Si absorption layer, the resultant higher power supply voltage for charge transfer may increase power consumption; therefore, it is challenging to design a high-performance silicon pixel for PDAF under near-infrared-ray incidence.

Pupil division due to selective light trapping

The key concept of this work for PDAF is to perform pupil division by generating light trapping [3-4] selectively in a pixel according to incident angle, using inverted pyramid textured interfaces for diffraction (PTID) and a deep trench isolation (DTI). The sidewall of the DTI completely reflects the diffracted light by the PTID: the light trapping [3-4].

We demonstrate a novel PDAF technique for incident 850 nm plane wave using 400 nm base size inverted PTID [3-5]: the PTID are locally arranged on light receiving surface (LRS) of c-Si, as illustrated in Fig. 1 and Table 1. The present pixel is based on a back-side illuminated CMOS image sensor pixel with one photo diode for visible light: we arrange the pixel in Bayer format for an on-chip color filter (CF). The pixel pitch is 1.85 μm and the thickness of c-Si is around 3 μm. The PTID are formed in the c-Si (111) surface on (100) plane by a wet etching process [3-5]. The aspect ratio of the PTID is fixed at 0.7071 because of the facet angle between c-Si (111) and (100). The grooves of the PTID and DTI are then filled with passivation films.

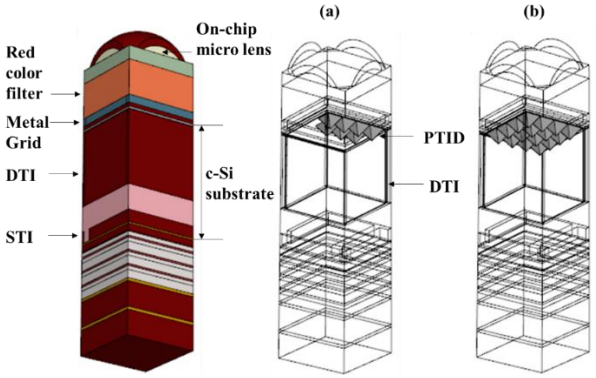

Figure 1. View from below of the present pixel for PDAF. Only the inverted pyramidal diffraction gratings including the Si (111) plane in the pixels (a) A and (b) B (shown in Table 1) are displayed, respectively.

Table 1. Investigated pixels.

pixel name		Cross section at metal grid	Cross section at light receiving surface
A	PTID arranged in the shape of T w/o LSF (proposed)	Red Color filter → Metal grid →	Crystalline silicon → PTID; DTI →
B	PTID arranged in 4 rows and 4 columns w/ LSF	Light shielding film (LSF) →	PTID; DTI →
C	No PTID w/ LSF (reference)	Light shielding film (LSF) →	Crystalline silicon → No DTI
D	No PTID w/o LSF	Green Color filter → Metal grid →	Crystalline silicon → No DTI
E	Same as the pixel A except PTID	Red Color filter → Metal grid →	Crystalline silicon → DTI →

Table 1 summarizes the investigated pixels. In the proposed pixel A with a red CF, we placed the PTID so that light with incident angles of +0° to +30° strikes the PTID. Moreover, we formed no metal LSF for pupil division, which avoids flare and ghost arising from the LSF; therefore, the present technique is different from the prior art categorized into three types: one half-shielding pixel [1], one pixel having two photo diodes [6] and two pixels sharing an on-chip micro lens [7].

The pixel A has neither a metal grid (MG) nor a DTI at the boundary with an adjacent pixel on the left: we omitted them to enhance EQE at an incident angle of +30°. The configuration of the pixels adjacent to the pixel A is the same except the on-chip CF; the DTI and MG of the adjacent pixels are arranged symmetrically with the pixel A in the Bayer format, but the PTID are placed at the same position as the pixel A.

In the pixel B with half metal-shielded aperture, the PTID arranged in 4 rows and 4 columns cover most region of the LRS. The reference pixel C with a flat LRS and half metal-shielded aperture is a current state-of-the-art pixel for PDAF [1]. The pixels D and E are used for correcting EQE ratio and contrast of the pixel A, which are relevant to the accuracy of AF. The pixel D has a flat LRS and an on-chip green CF. The pixels C and D have no DTI. The pixel E is same as the pixel A except for the PTID: it has a flat LRS.

Results and Discussion

We calculated the optical wave propagation in the pixels by rigorously solving the Maxwell's equations, using a three-dimensional finite difference time domain (FDTD) algorithm [8]; we considered both TE- and TM-polarized light and set periodic boundary condition corresponding to the Bayer format.

Figure 2 displays simulated angular response of power flux density distribution in the pixels (a) A and (b) C, respectively: the distribution under the propagation of TM-polarized light at the wavelength of 850 nm. Fig. 2 (c) illustrates the direction of TM polarization at normal incidence (+0°) for upper figures of Fig. 2 (a) and (b).

(a) pixel A (proposed) w/o metal LSF

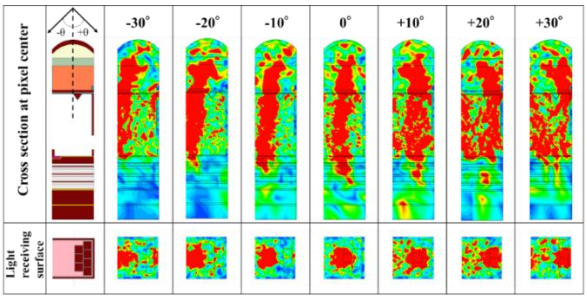

(b) pixel C (reference) w/ half metal-shielded aperture

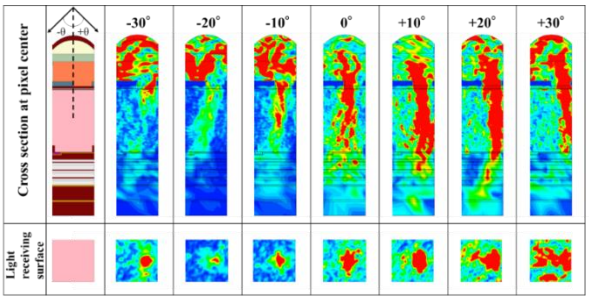

(c)

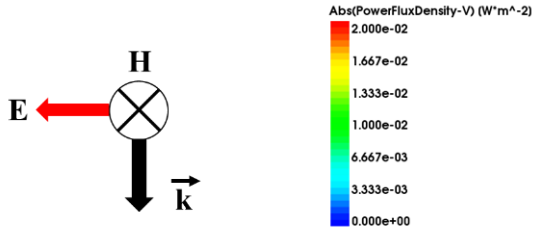

Figure 2. Simulated angular response of power flux density distribution by the propagation of TM-polarized light at the wavelength of 850 nm in the cross section at the pixel center (upper figure) and at the light receiving surface (lower figure) of (a) the proposed pixel A, (b) the reference pixel C, respectively; (c) direction of TM polarization at normal incidence (+ 0°) for upper figures of (a) and (b).

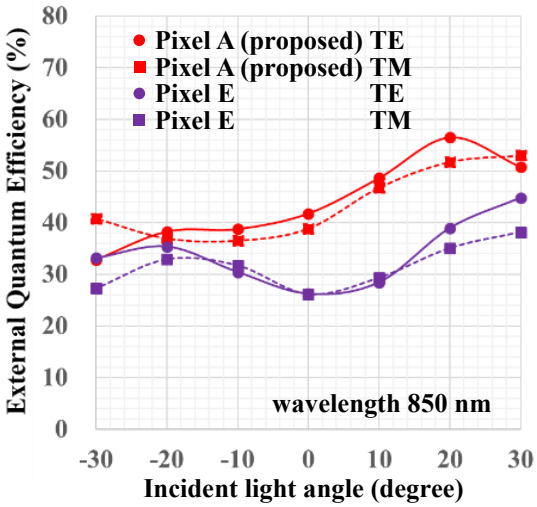

Figure 3. Simulated angular response of external quantum efficiency at the wavelength of 850 nm.

The pixel A shows that the incident light is diffracted by the PTID and then it is reflected at the sidewall of DTI for the incident angles of +0° to +30°; the resultant large spread of the distribution shows the light trapping [3-4]. On the other hand, the reference pixel C with half metal-shielded aperture exhibits smaller spread of the distribution for the same incident angles in comparison with that in the pixel A: no light trapping.

Figure 3 shows that the simulated angular response of the EQE behaves differently depending on the polarization; in the pixel E, reflection occurs on the sidewall of the MG for incident angles of +20° to +30°, so the difference in the EQE due to the polarization is clearly observed: the closer the angle of incidence on the sidewall approaches the Brewster angle, the greater the difference in the EQE due to the polarization. Thus, the average values of the EQE by the propagation of TE- and TM-polarized light for each incident angle are used in the following graphs for simplicity.

Figure 4 displays simulated angular response of the EQE for the pixels shown in Table 1. The EQE of the proposed pixel A exhibits above 36.8 % with the maximum of 54.2 %. On the other hand, the reference pixel C exhibits the EQE of 4.9 to 23.0 %. The pixel A exhibits 2.9 times improvement in the EQE at normal incidence compared to that of the pixel C; the EQE is 40.3 % and 13.8 %, respectively. The EQE in the pixel B is higher by 2 to 9 points compared to that in the reference pixel C because of the light trapping.

In order to evaluate the EQE gain by the selective light trapping, the EQE curves due to the difference between the pixels (A and D) and (A and E) are plotted in Fig. 5. The difference in the EQE between pixels A and E shows the EQE gains of 10.4 to 18.8 points for incident angles of +0° to +30°. In addition, the EQE curves due to the difference behave in the same manner as the EQE curve of the reference pixel C; therefore, that has numerically confirmed the validity of the pupil division due to the selective light trapping and the differential operation.

Surface texturing for solar cells reduces the optical reflection losses to well below 10 %, compared to a polished silicon surface which reflects about 30 % of the incident light in the visible region [3]. To allow a quantitative comparison between the inverted pyramid cell and the planar cell, their reflectance at each incidence angle were calculated in the same simulation [8].

Figure 6 displays simulated EQE as a function of reflectance. The optical reflection loss in the pixels A, D and E with no LSF is below 17.4 %, and the EQE of those pixels is more than 20 %. The EQE of the pixel A with the PTID is higher than that of the pixel E with a flat LRS despite the same reflectance; therefore, the light trapping is the main factor for the EQE enhancement. The same is true for the comparison of the pixels B and C which have half metal-shielded aperture.

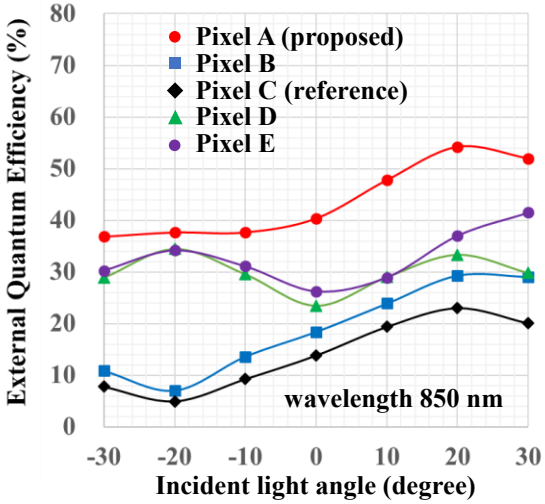

Figure 4. Simulated angular response of external quantum efficiency at the wavelength of 850 nm.

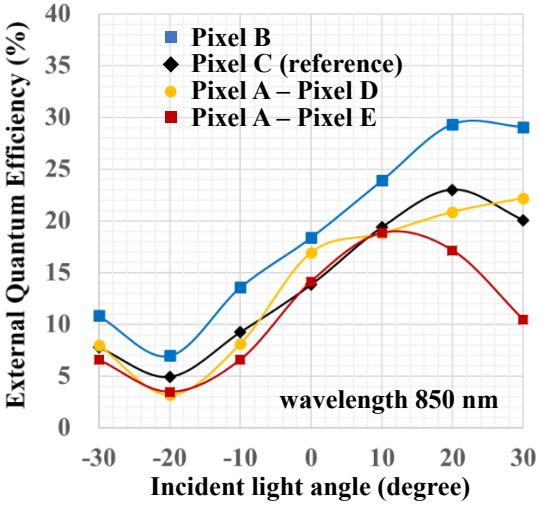

Figure 5. Evaluation of the simulated EQE gain due to the selective light trapping at the wavelength of 850 nm.

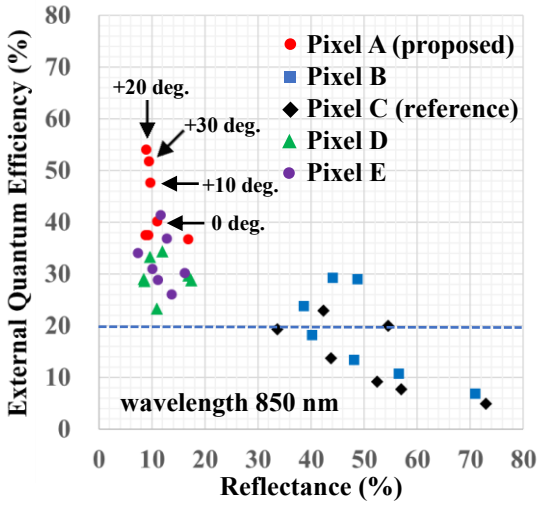

Figure 6. Simulated effective quantum efficiency as a function of reflectance at the wavelength of 850 nm.

Figures 7 and 8 show simulated angular response of normalized EQE ratio and the Michaelson contrast, respectively. The Michaelson contrast is defined by the following equation:

$$\text{Michaelson contrast} = \left| \frac{\Psi_{+\theta} - \Psi_{-\theta}}{\Psi_{+\theta} + \Psi_{-\theta}} \right|$$

$\Psi_{+\theta}$: EQE at incident light angle $+\theta$

$\Psi_{-\theta}$: EQE at incident light angle $-\theta$

The characteristics of the EQE ratio and the contrast of the pixel A deviates from those of the reference pixel C. To correct the deviation, the EQE ratio and the contrast subjected to the same differential operation as that in Fig. 5 were executed. The curves based on the difference operation behave in the same manner as the reference curves, showing that the same effect as the pupil division by LSF is obtained by the selectively arranged PTID, DTI and the differential operation.

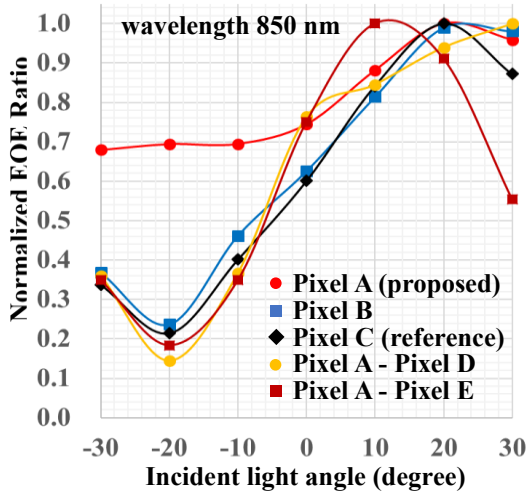

Figure 7. Simulated angular response of normalized quantum efficiency ratio at the wavelength of 850 nm.

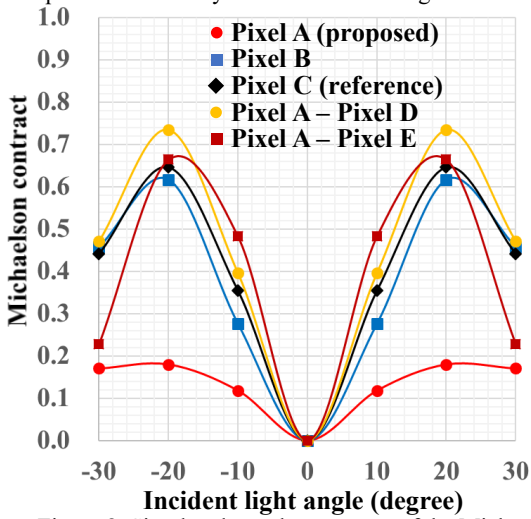

Figure 8. Simulated angular response of the Michaelson contrast at the wavelength of 850 nm.

Conclusions

A novel PDAF technique for incident 850 nm plane wave is demonstrated using 400 nm base size inverted pyramid textured interfaces for diffraction (PTID) with no separation, which are locally arranged on light receiving surface (LRS) of crystalline silicon (c-Si). No metal light shielding film for pupil division is formed. The key concept of this work for PDAF is to perform the pupil division by generating light trapping selectively in a pixel according to incident angle. The present pixel is based on a back-side illuminated CMOS image sensor pixel; the pixel pitch is 1.85 μm and the thickness of c-Si is around 3 μm. The FDTD simulation shows that the external quantum efficiency (EQE) of the present pixel exhibits above 36.8 % with the maximum of 54.2 % for incident angles from -30° to +30°, owing to the selective light trapping; it exhibits 2.9 times improvement in EQE at normal incidence compared to that of current state-of-the-art pixel with a flat LRS and half metal-shielded aperture: the EQE is 40.3 % and 13.8 %, respectively. By taking the difference from the EQE of the similar pixel except for the PTID, the characteristic curve of the present pixel behaves in the same manner as that of the current state-of-the-art pixel; therefore, that has numerically confirmed the validity of the pupil division due to the selective light trapping and the differential operation.

References

[1] R. Fontaine, "The State-of-the-Art of Mainstream CMOS Image Sensors," Proc. of International Image Sensor Workshop (IISW), 2015.

[2] M. A. Green, "Self-consistent optical parameters of intrinsic silicon at 300 K including temperature coefficients," Solar Energy Materials and Solar Cells, vol. 92, pp. 1305–1310, 2008.

[3] S. Sivasubramaniam, M. M. Alkaisi, "Inverted nanopyramid texturing for silicon solar cells using interference lithography," Microelectronic Engineering, 119, pp. 146-150, 2014.

[4] S. Yokogawa, I. Oshiyama, H. Ikeda, Y. Ebiko, T. Hirano, S. Saito, T. Oinoue, Y. Hagimoto, H. Iwamoto, "IR sensitivity enhancement of CMOS Image Sensor with diffractive light trapping pixels," Scientific Report, vol. 7, Art. no. 3832, 2017.

[5] I. Oshiyama, S. Yokogawa, H. Ikeda, Y. Ebiko, T. Hirano, S. Saito, T. Oinoue, Y. Hagimoto, H. Iwamoto, "Near-infrared Sensitivity Enhancement of a Back-illuminated Complementary Metal Oxide Semiconductor Image Sensor with a Pyramid Surface for Diffraction Structure," International Electron Devices Meeting (IEDM), Tech., Dig., pp. 397-400, 2017.

[6] M. Kobayashi, M. Johnson, Y. Wada, H. Tsuboi, H. Takada, K. Togo, T. Kishi, H. Takahashi, T. Ichikawa, S. Inoue, "A Low Noise and High Sensitivity Image Sensor with Imaging and Phase-Difference Detection AF in All Pixels," ITE Trans. on Media Technology and Applications (MTA), Vol.4, No. 2, pp. 123-128, 2016.

[7] WIPO Pub. No. WO2016/09864.

[8] Synopsys, 2016.